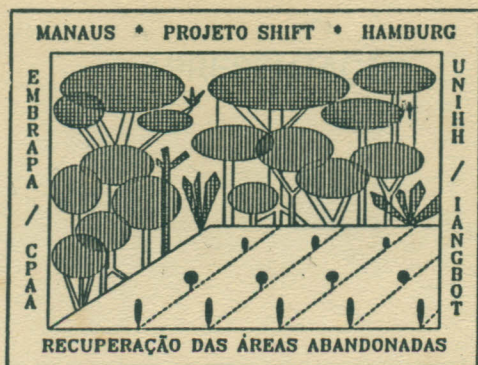


7120  
Schroth



# RECUPERAÇÃO DE ÁREAS DEGRADADAS E ABANDONADAS, ATRAVÉS DE SISTEMAS DE POLICULTIVO

634.99  
S555r  
1996


Período: Agosto/1992 - Março/1996

EMBRAPA/CPAA - Universidade de Hamburg

Editores:  
L. Gasparotto & H. Preisinger

634.99  
S555r  
1996  
1 ex.  
RT-2002.00241

MANAUS-AM  
Junho/1996

Recuperação de áreas  
1996 RT-2002.00241  
  
7720-1

## CLIMATOLOGICAL OBSERVATIONS RECORDED DURING THE PERIOD 1993 TO 1995 AT SHIFT PROJECT SITE IN MANAUS, CENTRAL AMAZÔNIA.

Oswaldo M.R.Cabral

**Abstract** - Hourly averages of solar and net radiation, air temperature and humidity, wind speed and direction, and soil temperatures were collected during the years 1993 to 1995 at SHIFT project site in Manaus. The variation of weather variables was similar to those obtained before in a clearing (Bastable *et al.*, 1993), and their daily ranges were several times the seasonal variation of the monthly averages. Annual totals of precipitation recorded were above the 1971-1993 period mean (2500mm), and the accumulated potential evaporation (Penman), was 40% of total rainfall. However, during the dry season months the vegetation established on the clay soil which covers the area probably experienced moderate soil moisture deficits wether its root system was not able to extract water below 1m depth.

### Introduction

The earth atmosphere is continuously absorbing heat at all latitudes, which comes from its surface, except near the poles. As no part of the system warms or cools noticeable over a period of a year, a two-way heat transfer from surface to the atmosphere and from equator to the poles must exist (Sellers, 1965).

The Amazon Basin is a region approximately 2000 x 2000 Km containing one of the world's largest rain forests (Paegle, 1987). It is one of the two or three large-scale tropical areas, where the high air temperatures and humidities promote the release of noticeable amounts of latent heat during the turbulent diffusion into the atmosphere. The region is convectively active at any given time, and thus its contribution is important to the global atmospheric cycle.

The differential heating between continent and ocean induces mass divergence (High) at upper tropospheric levels. During the Southern Hemisphere summer (December-March), the High is well developed and the effects are the enhancement of convection and the wet season establishment. When the High weakens and moves progressively northwestward (June-September), the southern and eastern sectors of the Basin experience their dry season, which can last between two months in central areas, to six months in the east and south regions (Molion, 1990).

Rainfall totals range from 1500mm to 3000mm annually, averaging about 2000mm in the Central Amazon. In the eastern and western ends of the Basin rains occur frequently throughout the year, whereas in the central part and in a portion of the western area of the basin there is a definite drier period (Salati & Vose, 1984).

The amount of solar energy received at the top of the atmosphere, which is the driven force of all processes occurring in the biosphere-atmosphere system, is a function of the latitude and day of the year. It varies near the Equator (3° S) from 30 MJm<sup>-2</sup> in June to 40MJm<sup>-2</sup> in January (Liou, 1980). For the same months the energy received at 45°N falls between 40 and 15 MJm<sup>-2</sup>, respectively. Besides the same energy load received in the tropics during the summer (January), when it is compared with mid-latitudes, factors as cloud cover and rainfall

counterbalance this potential and a decrease in the average temperatures during the rainy season is observed, as the maximum temperatures are kept lower (Riehl, 1965).

Although the monthly averages of air temperatures and humidities do not exhibit a marked variation (2°C and 20%) as does the precipitation, on a daily basis their amplitudes can be several times higher. Therefore a careful distinction between overcast and clear days must be done, as well between dry and wet seasons in order to completely understand the complex relationships occurring in the soil-plant-atmosphere system, particularly in the tropical region.

### Materials and Methods.

The climatological data were recorded by two stations: a conventional established in 1971 at EMBRAPA (2° 51 'S; 59° 52'W) main site, 30 Km northeast of Manaus; and by an automatic weather station (Didcot U.K.), installed in 1994, at the center of the SHIFT project area, 2 Km far from the former station.

At the conventional station (CS) the following data were available: daily average, maximum and minimum air temperatures; average humidities; 24h totals of rainfall; sunshine hours; evaporation (Piche evaporimeter); wind speeds and soil temperatures at 5cm, 10cm and 30cm depths.

The automatic weather station (AWS) recorded hourly averages of air temperature and humidity; solar and net radiation; wind speed and direction; soil temperatures at 5cm, 10cm and 30cm depths.

For some periods the AWS was not in operation and these gaps were filled by estimates based on CS data, through adjusted relationships between both data sets, as discussed below.

The correlation of air temperatures from ES and AWS showed that the average value calculated at ES can be utilized directly.

Daily totals of solar (Solar) and net (Net) radiation ( $\text{MJm}^{-2}$ ) when not available have been estimated through the daily number of sunshine hours (Sh), or via solar radiation as in the case when only net radiation data were missing, as follows:

$$\text{Solar} = 0.95 * \text{Sh} + 5.8 \quad R^2 = 0.61 \quad (1a)$$

$$\text{Net} = 0.61 * \text{Sh} + 5.7 \quad R^2 = 0.48 \quad (1b)$$

$$\text{Net} = 0.62 * \text{Solar} - 0.08 \quad R^2 = 0.89 \quad (1c)$$

During the periods when the humidity was not recorded at AWS site it has been estimated from CS daily mean as follows:

$$\text{RH}_{\text{AWS}} = 0.865 * \text{RH}_{\text{CS}} + 10.65 \quad R^2 = 0.79$$

This correction came from the comparison between 24 hours averages and the averages based on measured humidities at 8, 14 and 20 h (local time) obtained at CS, given by:

$$\text{RH}_{\text{CS}} = (\text{RH}_8 + \text{RH}_{14} + 2 * \text{RH}_{20}) / 4$$

## Results and Discussion

### Precipitation.

The mean monthly totals of rainfall from 1971 to 1993, and the data obtained from 1993 to 1995 are shown in Table 1. The wettest and driest months on the average were April ( $296 \pm 300$ mm) and August ( $104 \pm 50$ mm).

The annual totals recorded during the three years covered by this report were above the average (2503mm), which would induce to classify them as wet years. However, the conclusions based on such data can be misleading (Jackson, 1977), because the totals did not exhibit the temporal variability as showed by the standard deviations of April and August averages.

The number of rainy days in association with the monthly totals can be a useful indicative of dryer or wetter conditions, as noticed during August and October of 1995, when the amounts of rainfall recorded (30mm and 123mm) although not significantly lower than the averages, displayed a reduced the number of rainy days (7 and 6), which contrasted with the preceding years. If the same amount of precipitation fell in fewer days, probably their intensity was greater, which may promote dryer periods.

### Solar and net radiation.

The observed mean monthly totals of solar and net radiation fluxes are in Table 2. Although the amount of solar energy received at the top of the atmosphere is higher in January ( $40 \text{ MJm}^{-2}$ ), the average values observed at surface represented less than 40% of them, because the cloud cover at this time is intensified. The opposite situation was found during the dry season, when besides the minor potential ( $30 \text{ MJm}^{-2}$ ), 50% of it reaches the surface as less cloudy conditions are observed due to the reduced number of rainy days, agreeing with Salati & Marques (1984).

The net all wave radiation mean totals follow the solar radiation and precipitation pattern as well, and the higher values observed during the dry season are consequence of higher surface temperatures. On the average these totals represented approximately 60% of the solar radiation, which imply in losses of 40% via surface reflexion and net long-wave balance.

Horly averages of solar and net radiation fluxes are showed in Figure 1, during the beginning of rainy season (27 and 28 of November), when 19mm and 53mm of rainfall were recorded, and at dry season (3 and 4 of August), for comparison. The wet period is typified by the succession of clear and rainy days, when the fluxes can reach nearly the same values as the observed during the dry period and on the following day a dramatic decrease due to rainfall and cloud cover.

The totals of solar radiation recorded during the time sequence presented in Figure 1 were 16, 2.5, 19 and 17  $\text{MJm}^{-2}$ , and the corresponding net radiation were 12, 1.5, 13 and 11  $\text{MJm}^{-2}$ .

### Air temperature.

The annual course of solar radiation which reaches the surface and the vegetation characteristics as its biomass, and spectral properties determine the air temperature averages showed in Figure 2. The mean values range was 24 to 26 °C, and the differences between maxima (29 to 35 °C) and minima (20 to 23 °C) were approximately 10°C, which gives the order of daily amplitudes usually found.

Hourly values of air temperature obtained during the same wet and dry periods of radiation section are presented in Figure 3. The daily averages were 26.7, 23.8, 26.3 and 25.7 °C, and the maxima and minima were (22.9-32.6), (22.8-25.0), (19.2-36.2) and (20.6-36.4)°C. The lower average during the rainy day follows the lower maximum (day 2), as stated before, and the lower minima observed during the dry season are the result of clear nights, usually, but eventually can be promoted by strong cold fronts, which arrive the region during the Southern Hemisphere winter.

### Soil temperature.

Mean monthly averages of soil temperatures at 5, 10 and 30cm depths, and totals of precipitation are in Figure 4. The 1993 data were measured at CS, and display a greater scatter when it is compared with the following years. This irregular behaviour is mostly consequence of how daily averages were calculated, based on soil temperatures records acquired three times a day.

The observed range was 25-28°C, corresponding to the wet and dry periods. The poor definition between depths at this time scale reflects the fact that they tend to the same average value.

The heat flow in soil depends on its thermal properties which may change profoundly as its water content and or compaction occur (Monteith, 1973). Hourly averages of soil temperatures showed in Figure 5, are examples of the modification of thermal regimes as a function of the water content. Although the solar energy received during the first day was similar to the last two days (see Figure 1), their amplitudes differ significantly. The higher soil moisture storage at the surface layer (10cm) probably increased the thermal conductivity, which contrasts with the lower soil temperatures during the dry season, as probably most of the soil micropores are empty.

Many biological processes depend on soil temperature: the metabolism and behaviour of microorganisms and many invertebrates; the germination of seeds and extension of root systems are examples of such links (Monteith, 1973), which can only be detected if hourly data, as presented here is available, and consequently the biological processes sampling follows the same time scale.

### Air humidity

Relative humidities and air temperatures time series are presented in Figure 2. The mean humidities range was 80 to 93%, and the corresponding air temperatures interval was 24 to 26 °C. The same relative humidity represents at different air temperatures different amounts of

water vapor in the air, therefore to avoid confusion the temperature should be specified whenever relative humidity is used (Zadoks & Schein, 1979).

The air humidity is better expressed through the specific humidity and saturation deficits (Figure 6), which represent the absolute content of water vapour in the air; their ranges were 16 to 19 g kg<sup>-1</sup>, and 2 to 4 g kg<sup>-1</sup>, respectively. On a daily basis (Figure 3), the deficits varied between saturation overnight (i.e. zero) and reached 13 g kg<sup>-1</sup> or three times the annual amplitudes, whose average deficits never reached the saturation, even during the wettest periods.

Whereas it is only recently that the response of stomatal conductance ( $g_s$ ) to humidity deficit has been investigated for tropical vegetation, existing results indicate that many plants show a similar response to those of temperate species (Roberts *et al.*, 1990). In their study the authors found that the response of  $g_s$  to humidity deficit was more sensitive when the radiation was high, but a higher sensitivity was also observed for wettest soil.

#### Wind speed.

Monthly averages of wind speed are in Figure 7, which shows a steady flow of 0.3ms<sup>-1</sup>. However, as reported by Bastable *et al.* (1993), in a clearing, during the day the wind speeds recorded (1.6ms<sup>-1</sup>) may be comparable with those over the forest (Figure 8), but at night the wind speed falls below the resolution of the anemometer. The wind direction is also presented in Figure 4a, and for most of the time it is predominantly easterly (90 degrees).

The reduction of the wind speed at night indicates that there is a strong thermal inversion, whose effect is to decouple the near-surface wind from that of the atmosphere above. Under such circumstances, the minimum temperatures should be lower than those observed during windy or cloudy nights.

The lower nocturnal ventilation associated with saturated air promote ideal conditions for dew and fog formation on the plant leaves which may facilitate spore germination and the growth of parasitic fungi and diseases (Bastable *et al.*, 1993).

#### Potential evaporation.

The potential evaporation (PE) estimates were based on Penman method (Shuttleworth *et al.*, 1984), accordingly to:

$$PE = [ D \cdot R_n + r \cdot c_p \cdot D \cdot f(u) ] / ( D + c_p / l ) \quad (4)$$

where

$$f(u) = 0.004 \cdot ( 1 + 0.54 \cdot u ) \quad (4a);$$

D is the slope of saturation vapour pressure curve at air temperature, l is the water latent heat,  $R_n$  is the integrated radiation input, D the daily average specific humidity deficit, and  $u$  the daily average wind speed (ms<sup>-1</sup>).

Figure 9 shows the time series of potential evaporation, precipitation and evaporation measured at CS (Piche evaporimeter). The ratio between accumulated PE (3035 mm) and precipitation (8277mm) was 0.37 during the three years, and the Piche totals (2125mm) were 30% lower than the PE estimates. On the average, the energy and aerodynamic terms of

equation 4 represented 92% and 8%, respectively, of the EP estimates, which is consistent with the small daily averages of humidity deficits and wind speeds, showed in the preceding sections.

Based on the overall ratio between PE and precipitation, approximately 40% of precipitation returns to the atmosphere via local evaporation, which is lower than the 50% estimated for natural forest (Shuttleworth *et al.*, 1987; Salati & Vose, 1984).

In the forest during the wettest months (February) the Penman equation underestimates the evaporation, as the method is not capable to quantify the enhanced evaporation by interception loss; and during the driest months (September) the evaporation was overestimated, because the method does not comprise the vegetation response to increasing soil water tension and a possible reduction in leaf area.

The Penman estimates for pasture land (Wright *et al.*, 1992) were always greater than measured evaporation and only just after rainfall tends to converge with measurements. Measured evaporation was typically 0.7-0.8 of Penman estimate, falling to 0.5-0.6 with increasing soil moisture stress.

The ratios between Penman estimates of evaporation and measurements reported by Wright in the grassland are similar to PE and Piche ratios, therefore the evaporimeter data can be representative of short vegetation evaporation, without soil moisture restrictions.

Although the accumulated PE represented 40% of the total precipitation, Figure 9 shows that during the dry season there are moderate soil moisture deficits. When the rainfall is lower than PE, as for example between July and September of 1993, the accumulated difference was -38.4 mm, and in August of 1995, the deficit was -80 mm.

The soil of SHIFT project area is classified as a yellow Latosol, whose clay content is above 80%. For this soil Cabral (1991), found that the (0-1)m layer stores approximately 40mm of available water. Based on the estimated deficit in 1995, greater than the available soil moisture capacity, the vegetation should have an active root system below 1m depth, in order to prevent or minimize water stress.

## Conclusions.

The variation of weather variables was similar to those obtained before in a clearing (Bastable *et al.*, 1993), and their daily ranges were several times the seasonal variation of the monthly averages.

The soil temperature amplitudes differed significantly when the soil was wet or dry. The higher soil moisture storage at the surface layer (10cm) probably increased the thermal conductivity, which contrasted with the lower soil temperatures during the dry season, as probably most of the soil micropores were empty.

Annual totals of precipitation recorded were above the 1971-1993 period mean (2500mm), and the accumulated potential evaporation (Penman), was 40% of total rainfall. However, during the dry season months the vegetation established on the clay soil which covers the area probably experienced moderate soil moisture deficits wether its root system was not able to extract water below 1m depth.

## References

- Bastable, H. *et al.* 1993. Observations of climate, albedo, and surface radiation over cleared and undisturbed Amazonian forest. *Int.J.Climatology*, 13, 783-796.
- Cabral, O.M.R. 1991. Armazenagem de água num solo com floresta de Terra-Firme e com seringal implantado. Tese de Mestrado, INPE, São José dos Campos, 104p.
- Jackson, I.J. 1977. Climate, water and agriculture in the tropics. New York, Longman, 248 pp.
- Liou, K.N. 1980. An introduction to atmospheric radiation. New York, Academic Press, 392 pp.
- Molion, L.C.B. 1990. Climate variability and its effects on Amazonian hydrology. *Interciencia*, Vol.15(6), 367-372.
- Monteith, J.L. 1973. Principles of environmental physics. London, Edward Arnold, 241 pp.
- Paegle, J. 1987. Interactions between convective and large-scale motions over Amazônia. In: Dickinson, R.E. ed., *The Geophysiology of Amazônia*. New York, John Wiley, p. 347-390.
- Roberts, J.M., Cabral, O.M.R. & Aguiar, L.F. 1990. Stomatal and boundary-layer conductances in an Amazonian terra-firme rainforest. *J.Appl.Ecology*, 27: 336-353.
- Salati, E. & Marques, J. 1984. Climatology of the Amazon region. In: Siole, H. ed., *The Amazon: Limnology and Landscape ecology of a mighty tropical river and its basin*. Dordrecht, Dr. W. Junk Publishers, 85-126.
- Salati, E. & Vose, P.B. 1984. Amazon Basin: A system in equilibrium. *Science*, 225(4658), 129-138.
- Sellers, W.D. 1965. Physical Climatology. University of Chicago Press, 350 pp.
- Shuttleworth, W.J. *et al.* 1987. Amazonian Evaporation. *R. Bras. de Meteorologia*, Vol.2, 179-191.
- Shuttleworth, W.J. *et al.* 1984. Eddy correlation measurements of energy partition for Amazonian forest. *Q.J.R. Meteorol.Soc.*, 110: 1143-1162.
- Riehl, H. 1965. Meteorologia Tropical. Rio de Janeiro, Ao Livro Técnico, 426 p.
- Zadocks, J.C & Schein, R.D. 1979. Epidemiology and plant disease management. New York, Oxford University Press, 427 pp.
- Wright, I. *et al.* 1992. Dry season micrometeorology of central Amazonian ranchland. *Q.J.R.Meteorol.Soc.*, 118, 1083-1099.



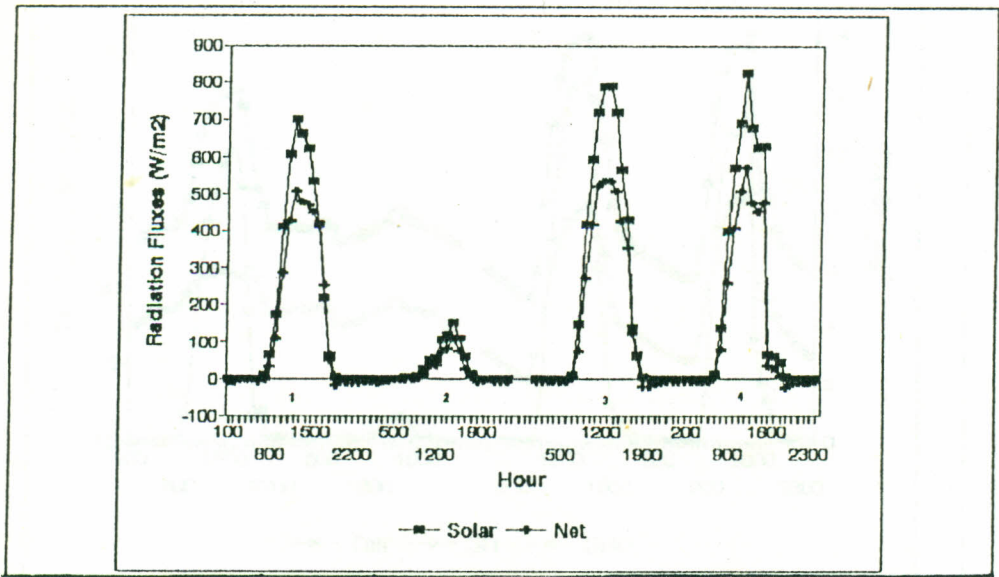


FIG. 1- Hourly fluxes of solar and net radiation.

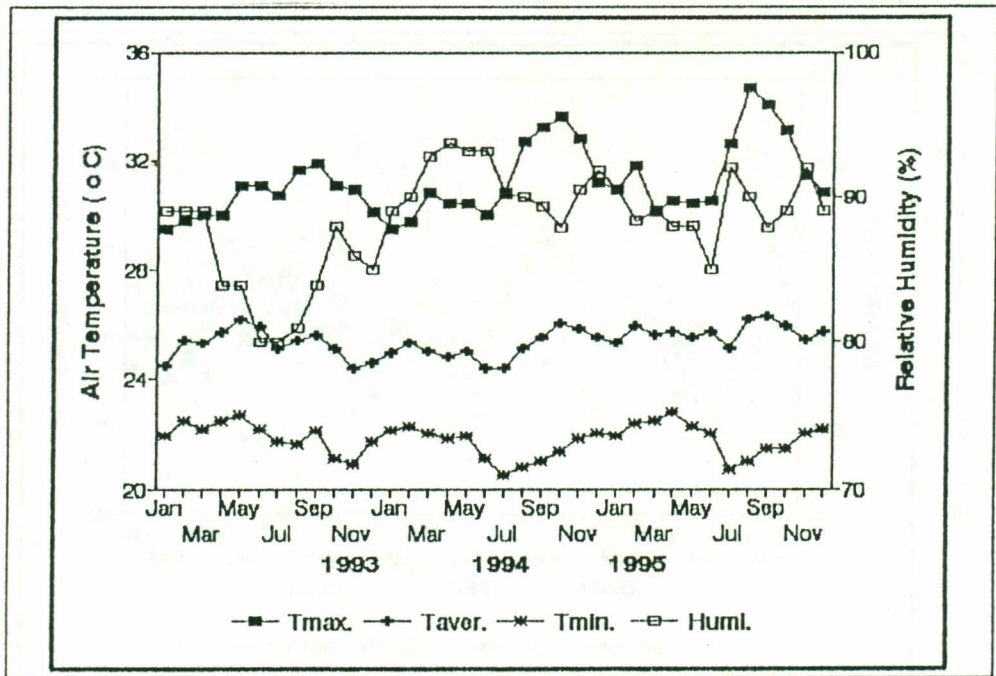


FIG 2 - Monthly averages of air temperature and relative humidity.

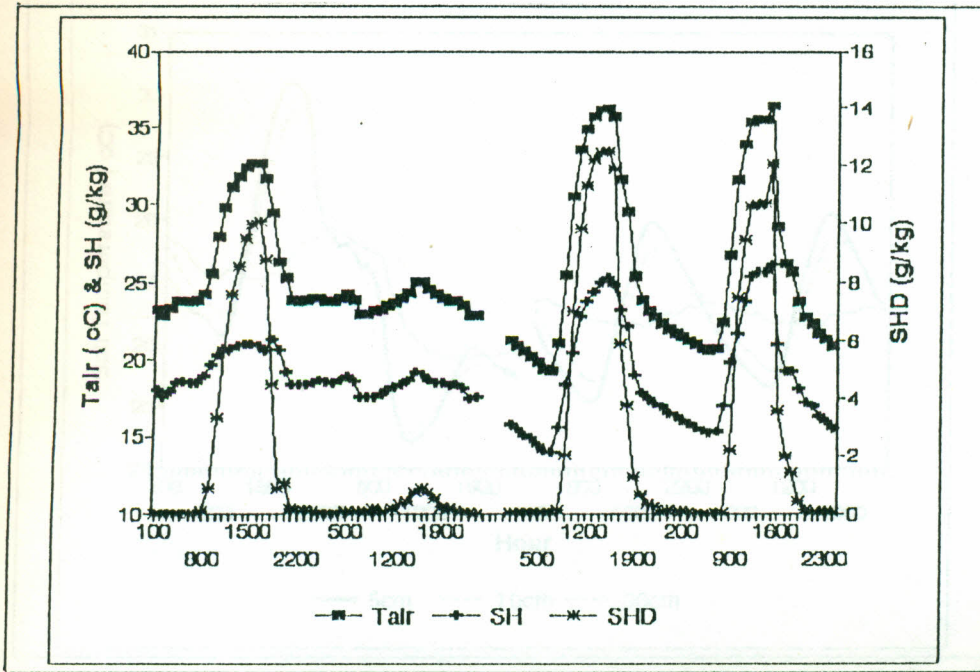


FIG 3 - Hourly averages of air temperature, specific humidity and specific humidity deficit.

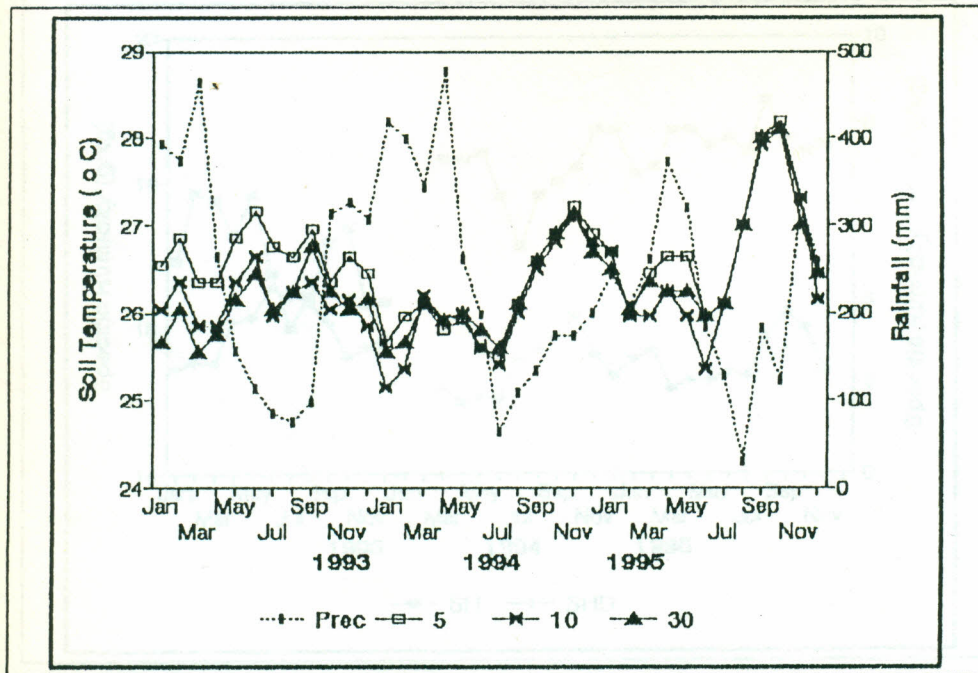


FIG 4 - Monthly averages of soil temperature at 5, 10 and 30cm depths, and monthly totals of precipitation.

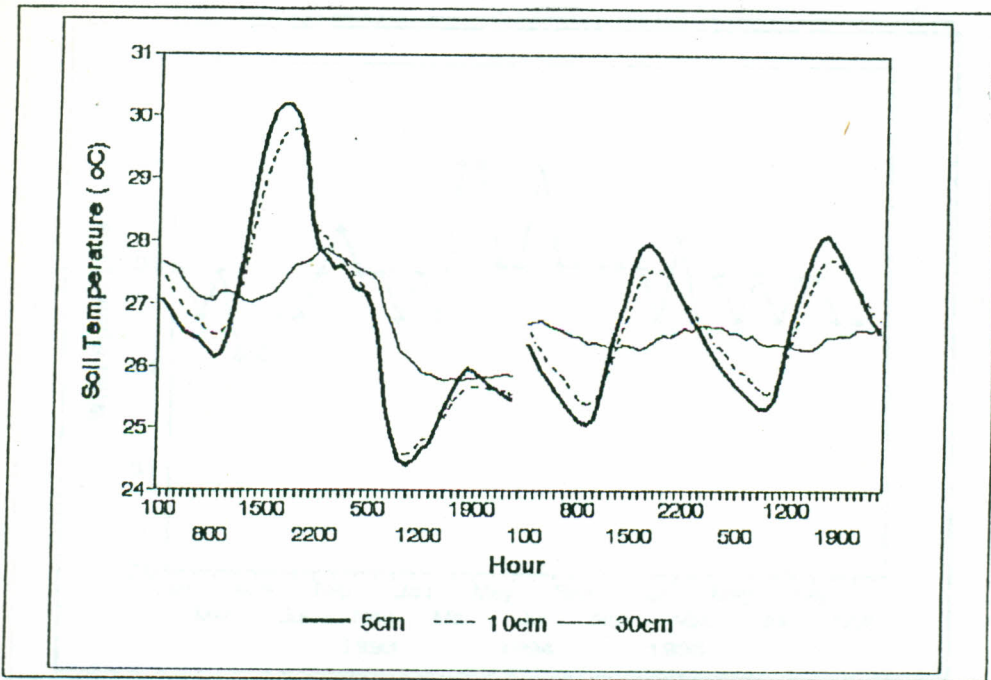


FIG 5 - Hourly averages of soil temperature at 5, 10 and 30cm depths.

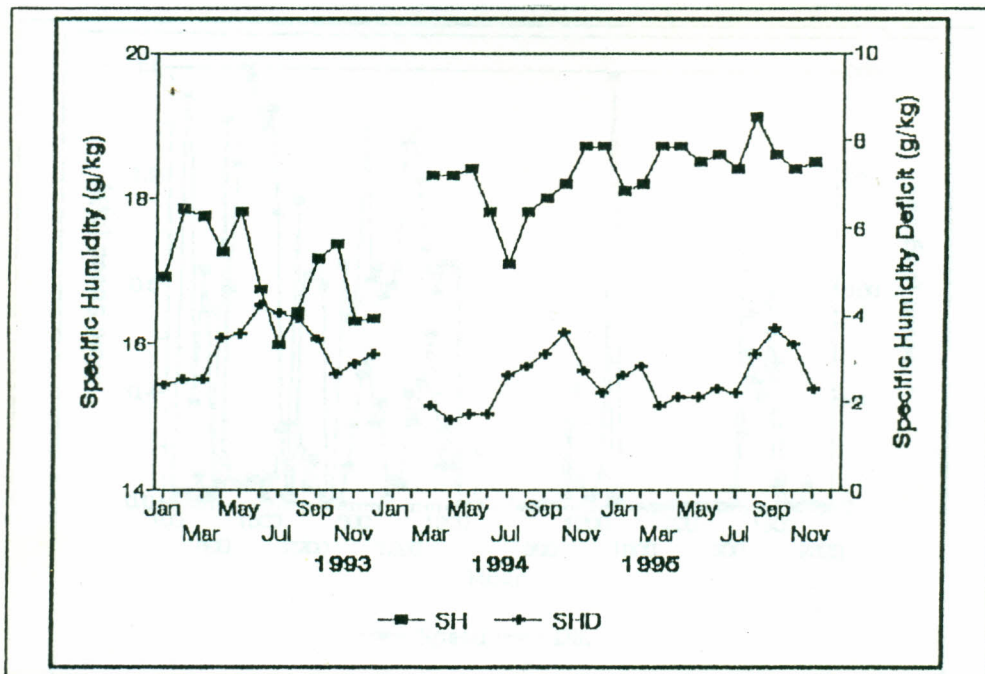


FIG 6 - Monthly averages of specific humidity and specific humidity deficit.

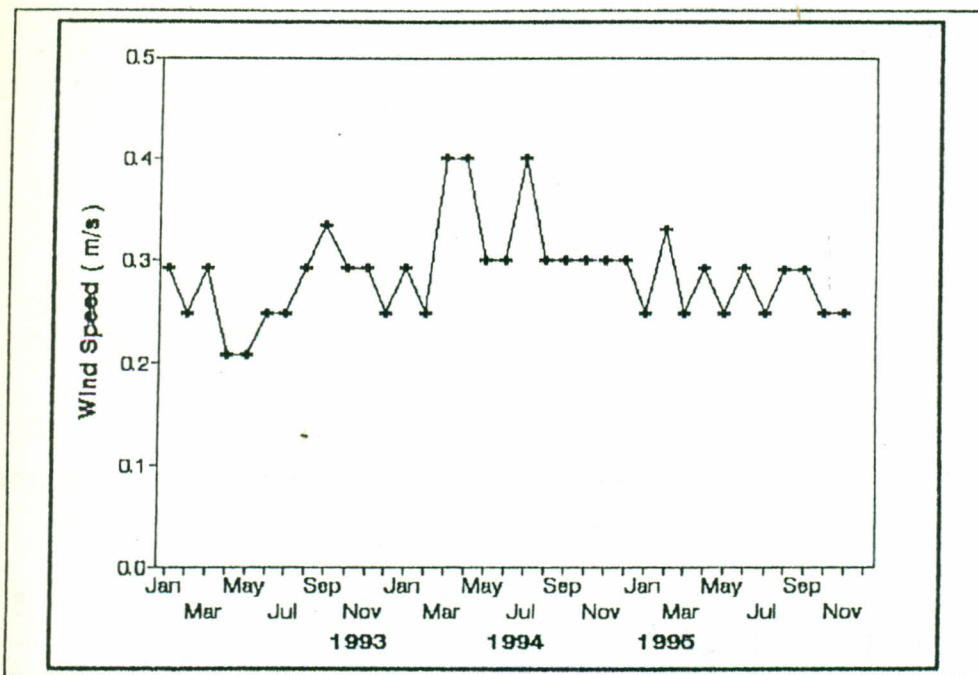


FIG 7 - Monthly averages of wind speed.

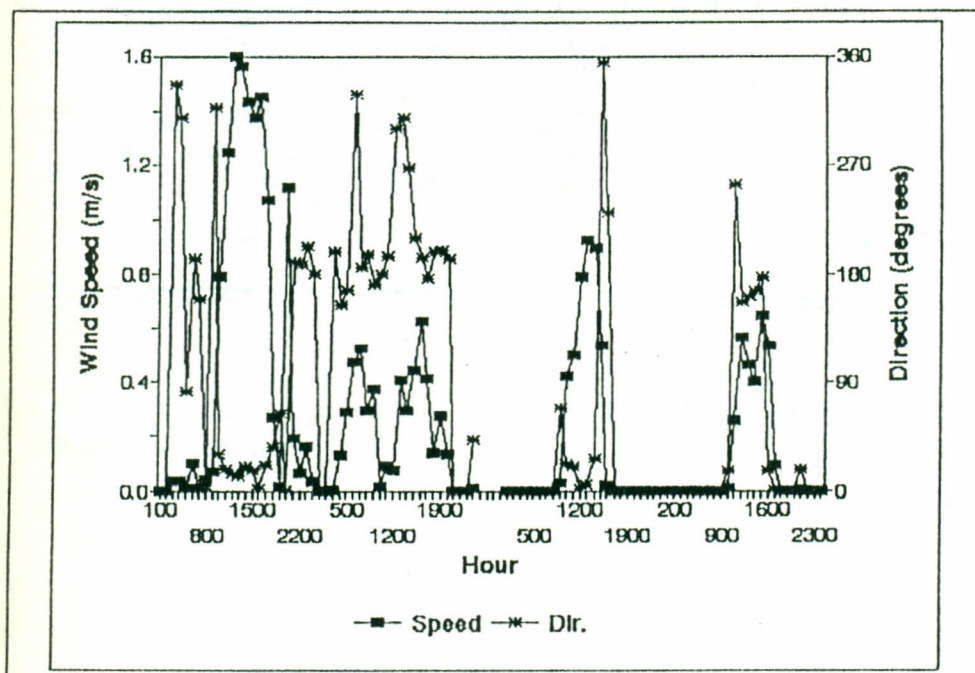


FIG 8 - Hourly averages of wind speed and wind direction.

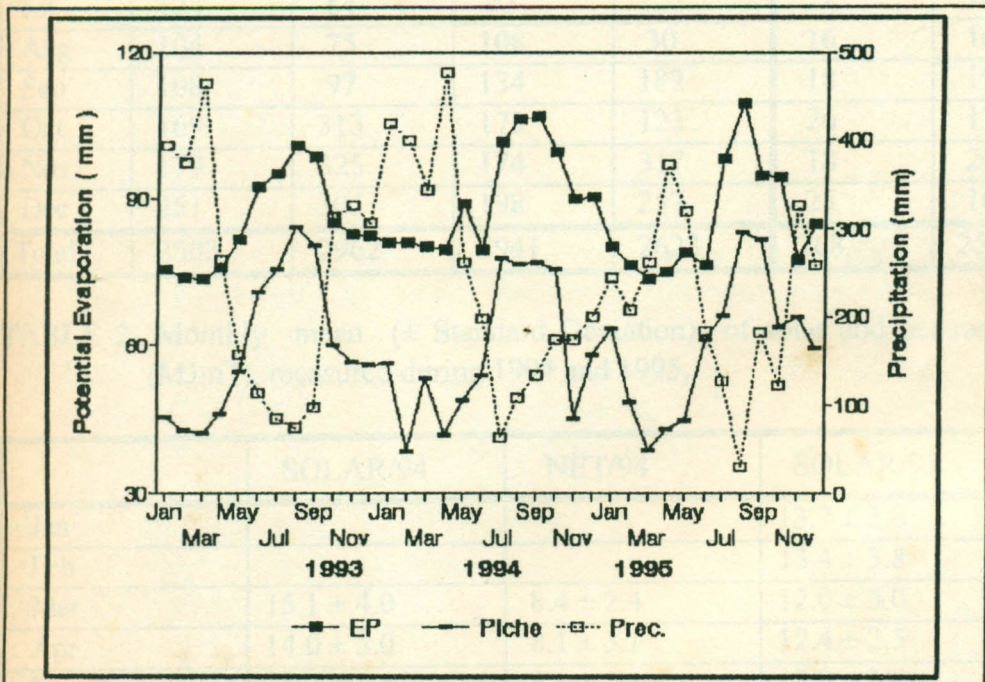


FIG 9 - Monthly totals of potential evaporation (PE), precipitation and actual evaporation (Piche evaporimeter).

TABLE 1- Averages for 1971-1993 period and monthly totals of precipitation, and number of rainy days.

	71-93	1993	1994	1995	1993	1994	1995
	mm	mm	mm	mm	----	-days-	-----
Jan	262	392	417	243	22	25	15
Feb	289	373	398	208	24	23	13
Mar	288	464	342	262	27	26	22
Apr	296	265	476	372	26	28	17
May	276	156	261	319	21	26	24
Jun	155	113	197	183	23	25	16
Jul	124	84	63	127	22	13	15
Aug	104	75	108	30	16	16	7
Sep	108	97	134	182	18	19	10
Oct	169	313	173	123	26	17	6
Nov	179	325	174	317	18	20	19
Dec	251	305	198	257	25	16	21
Total	2503	2962	2941	2623	268	254	185

TABLE 2- Monthly mean ( $\pm$  Standard Deviation) of solar and net radiation daily totals ( $\text{MJm}^{-2}$ ), measured during 1994 and 1995.

	SOLAR/94	NET/94	SOLAR/95	NET/95
Jan			13.2 $\pm$ 3.0	9.4 $\pm$ 1.0
Feb			13.4 $\pm$ 3.8	9.3 $\pm$ 3.0
Mar	15.1 $\pm$ 4.0	8.4 $\pm$ 2.4	12.0 $\pm$ 3.0	7.4 $\pm$ 1.9
Apr	14.0 $\pm$ 5.0	8.1 $\pm$ 3.1	12.4 $\pm$ 2.5	7.6 $\pm$ 1.6
May	14.4 $\pm$ 3.5	8.8 $\pm$ 2.4	12.9 $\pm$ 3.0	7.9 $\pm$ 1.9
Jun	13.2 $\pm$ 3.6	8.2 $\pm$ 2.5	12.7 $\pm$ 3.6	7.8 $\pm$ 2.2
Jul	15.6 $\pm$ 4.1	9.9 $\pm$ 2.8	14.3 $\pm$ 2.9	9.9 $\pm$ 2.1
Aug	16.5 $\pm$ 3.6	10.2 $\pm$ 2.4	16.0 $\pm$ 2.2	10.8 $\pm$ 1.6
Sep	16.6 $\pm$ 3.3	10.5 $\pm$ 2.2	15.4 $\pm$ 3.6	9.3 $\pm$ 2.2
Oct	17.0 $\pm$ 3.6	9.2 $\pm$ 2.1	14.1 $\pm$ 4.0	9.2 $\pm$ 3.0
Nov	14.1 $\pm$ 4.0	8.4 $\pm$ 2.7	11.8 $\pm$ 4.5	8.8 $\pm$ 3.0
Dec	12.5 $\pm$ 4.3	8.9 $\pm$ 3.3		
average*	13.5	8.8	14.9	9.1
maximum*	20.0	14.3	22.2	14.2
minimum*	2.4	2.5	2.2	0.9

\* overall daily totals